pagepress

Inner-ear circulation in humans is disrupted by extracranial venous outflow strictures: Implications for Ménière's disease

Eleuterio F. Toro,[1] Francesco Borgioli,[1] Qinghui Zhang,[1] Christian Contarino,[2] Lucas Omar Müller,[1,3] Aldo Bruno[4]

[1]Laboratory of Applied Mathematics, DICAM, University of Trento, Trento, Italy; [2]Department of Mathematics, University of Trento, Povo (TN), Italy; [3]Biomechanics Group, Department of Structural Engineering, NTNU, Trondheim, Norway; [4]Vascular Surgery Division, Gepos Clinic, Telese Terme (BN), Italy

Abstract

Ménière's disease (MD) is a pathology of the inner ear, the symptoms of which include tinnitus, vertigo attacks, fluctuating hearing loss, and nausea. Neither cause nor cure are currently known, though animal experiments suggest that disruption of the inner ear circulation, including venous hypertension and endolymphatic hydrops, to be hallmarks of the disease. Recent evidence for humans suggests a potential link to strictures in the extracranial venous outflow routes. The purpose of the present work is to demonstrate that the inner-ear circulation in humans is disrupted by extracranial venous outflow stricture and to discuss the implications of this finding for MD. The hypothesis linking extracranial venous outflow strictures to the altered dynamics of central nervous system (CNS) fluid compartments is investigated theoretically via a global, closed-loop, multiscale mathematical model for the entire human circulation, interacting with the brain parenchyma and cerebrospinal fluid (CSF). The fluid dynamics model for the full human body includes submodels for the heart, pulmonary circulation, arterial system, microvasculature, venous system and the CSF, with a specially refined description of the inner ear vasculature. We demonstrate that extracranial venous outflow strictures disrupt inner ear circulation, and more generally, alter the dynamics of fluid compartments in the whole CNS. Specifically, as compared to a healthy control, the computational results from our model show that subjects with extracranial outflow venous strictures exhibit: altered inner ear circulation, redirection of flow to collaterals,
increased intracranial venous pressure and increased intracranial pressure.

Our findings are consistent with recent clinical evidence in humans that links extracranial outflow venous strictures to MD, aid the mechanistic understanding of the underlying features of the disease and lend support to recently proposed biophysically motivated therapies aimed at reducing the overall pressure in the inner ear circulation. More work is required to understand the finer details of the condition, such as the associated dynamics of fluids in the perilymphatic and endolymphatic spaces, so as to incorporate such knowledge into the mathematical models in order to reflect the real physiology more closely.

Introduction

The potential link between anomalous strictures in the main extracranial venous outflow routes, alterations of the dynamics of the CNS fluid compartments, including venous hypertension, and CNS pathologies is becoming an active subject of interdisciplinary research. Alperin et al.[1] linked extracranial (as well as intracranial) venous outflow anomalies to Idiopathic Intracranial Hypertension (IIH). Zamboni et al.[2] associated extracranial venous outflow anomalies to Multiple Sclerosis (MS); they called the venous anomaly Chronic Cerebrospinal Venous Insufficiency (CCSVI). More recently, such venous strictures have been associated to MD, a pathology of the inner ear.[3-7] The present research is motivated by these recent works and by previous experiments on animals[8] and humans[9] that identify alterations of the inner ear circulation as a distinguishing feature of MD. We present results from a theoretical study that show how anomalous strictures in the main extracranial venous outflow routes cause chronic venous hypertension throughout the cerebral venous system, including the inner ear circulation. This study addresses the underlying biophysical mechanisms and provides a partial explanation for i) the empirical association between extracranial venous outflow strictures and MD, ii) the apparent success of reported clinical experience.

MD is a pathology of the inner ear. The inner ear houses and protects the neurological structures employed by the hearing (cochlear apparatus) and equilibrium functions (vestibular apparatus);[10,11] it is located in the petrous part of the temporal bone and consists of the external bony labyrinth and the internal membranous labyrinth. The space between these two surfaces is filled

with perilymph, a fluid whose ionic composition is similar to that of interstitial fluid (ISF) and cerebrospinal fluid (CSF), rich in sodium and calcium and poor in potassium. Perilymph is in contact with the CSF via the cochlear aqueduct, which drains the fluid towards the subarachnoid space. The membranous labyrinth contains endolymph, whose ionic composition is high in potassium, thus more comparable to intracellular fluid. Since production of endolymph is continuous, a constant removal from the inner ear is needed. The endolymphatic duct, the canal responsible for this function, runs within the vestibular aqueduct, from the central part of the membranous labyrinth to a terminal swelling known as the endolymphatic sac, which is located between two layers of dura mater and from which endolymph is reabsorbed into the subdural space.[12]

Arterial blood supply of the inner ear is provided by the labyrinthine artery, which usually branches from the anterior inferior cerebellar artery or, more rarely, directly from the basilar artery. The labyrinthine artery is in fact a set of arterioles, whose small diameters contribute to the attenuation of arterial pressure and intense blood

OPEN ACCESS

flow, thus ensuring smooth blood supply to the inner ear.[10,12] The inner ear venous blood drainage is provided essentially by three veins, subject to individual variability: i) The vein of the cochlear aqueduct (VCAQ), also known as vein of the cochlear canaliculus. This vein runs parallel to the cochlear aqueduct (endolymph), it drains the basal turn of the cochlea, the saccule and part of the utricle, and empties into the superior bulb of the internal jugular veins (IJVs). ii) The vein of the vestibular aqueduct (VVA) is another prominent vessel for venous drainage of the inner ear; sometimes, the anterior and posterior vestibular veins are present, and they all drain blood from the semicircular canals and the utricle, they merge into the VVA, which runs within the vestibular aqueduct and parallel to endolymphatic duct, and empties into the inferior petrosal sinus or in the jugular bulb. However these veins are not always present in the inner ear vasculature. iii) The labyrinthine vein (LABV), or internal auditory vein. Blood from the vestibular aqueduct is mainly drained by the LABV, which runs parallel to the labyrinthine artery, drains venules both from the cochlear and the vestibular apparatus and ends in the sigmoid sinus, in the superior petrosal sinus or in the transverse sinus. In this paper we shall assume subjects to lack the VVA, which is a possible anatomical variation.

MD is characterized by attacks of nausea, tinnitus, vertigo and fluctuating hearing loss. The normal onset of MD is unilateral, but the condition often extends to the other ear, with a registered 40% of bilateralization cases observed in the first 5 years.[5] Hearing loss is initially temporal, but frequently worsens to permanent, or severe deafness. The symptoms of MD are quite common and typical of many other pathologies. This means that the number of MD diagnosed patients is probably smaller than the effective number of MD diseased subjects. Historically, MD was first described in 1861 by the French physician Prosper Ménière, but its aetiology remains uncertain, up to now. Genetic factors, autoimmune mechanisms, environmental conditions, infection consequences and even iatrogenic or psychological causes have all been considered through many decades, without finding a strong or predominant correlation of any of these with MD. None of these factors have resulted to be a necessary and sufficient condition for the development of the disease.[13] As the origin of MD is uncertain, no universally accepted therapy for this pathology has so far been found.

In spite of these uncertainties, we believe that biophysical aspects may play an important role in altering the circulation of fluids in the inner ear. A persistent anomalous condition in the inner ear, called *endolymphatic hydrops*.[14-16] has been observed in MD patients; such condition is characterised by an increase of the endolymphatic volume and pressure in the *membranous labyrinth*. The causes of EH are still uncertain, but it seems reasonable to suggest that obstruction of the *endolymphatic sac*, or duct, produces a backlog of fluid in the *endolymphatic space*, which leads to the increase in volume and pressure. Moreover, it has recently been suggested that a potential origin of MD could be the altered cerebral venous flow caused by extracranial venous outflow strictures.[3-7]

The involvement of vascular mechanisms in MD has already been proposed in classical works.[14-16] Animal experimental research has strengthened the biophysical viewpoint.[8,9,17,18] A convincing demonstration of an association between anomalous extracranial blood outflow and MD could eventually lead to a well-documented and accepted treatment of MD patients; medical doctors have already made inroads in this direction,[3-7] with encouraging results. An understanding of the basic mechanisms at work would be useful to provide an explanation for these results and also for possibly optimising the procedures.

The first clinical studies of the potential link between MD and extracranial venous anomalies are quite encouraging. Di Berardino and collaborators[7] conducted a study on 52 subjects with cochleo-vestibular disturbances. The patients were divided into a first group of 24 patients diagnosed with unilateral MD and a second group of 28 subjects suffering from unilateral disturbances but not diagnosed as MD patients (not-MD). Magnetic resonance venography (MRV) and echo-color Doppler (ECD) were conducted on all subjects to examine the extracranial venous outflow. The MRV technique revealed anomalous venous drainage in 20 MD patients (83%) and in 16 not-MD (57%), while the ECD technique detected abnormalities in 15 MD cases (62%) and in 6 not-MD (21%). Most frequently, the observed anomalies were asymmetries of the outflow within IJVs and vertebral veins.

One of the first surgery treatments based on the assumed link between MD and CCSVI was reported by Bruno *et al*.[5] The first step in their procedure included a group of 50 MD diagnosed patients, who had previously undergone several conventional therapies, with no benefits. Their study also included a healthy control group of 100 subjects. In the MD group, 45 out of 50 (90%) were diagnosed with the CCSVI con-dition, while in the control group only 3 out of 100 subjects (3%) were found to be affected by CCSVI. In the 45 positive MD patients, 20 were also examined by means of venography that confirmed in all the cases, bilateral lesions in the IJVs and in three cases, also a lesion in the azygos vein (AV). At a later stage, these patients underwent bilateral percutaneous transluminal angioplasty (PTA) of the affected IJVs and the AV, aimed at enlarging the cross-sectional of the narrowed vessel and restoring venous outflow. Six months after the surgery, 19 out of 20 patients showed clear improvement of the symptoms, with more rare episodes of vertigo and higher hearing capacity; 1 patient out of 20 showed re-stenosed IJVs, which is known to be the disadvantage of PTA. A more recent work on the same topic is that of Bruno *et al*.[6]

The available animal experimental evidence, the indications of an association between MD and CCSVI conditions in humans as well as the encouraging results from surgical treatment using PTA, warrant a more detailed, quantitative study of the CCSVI link trying to identify the basic mechanisms at work. Measurements have revealed altered venous flow in CCSVI affected subjects and invasive pressure measurements in extracranial districts have confirmed the expected result of (local) venous pressure increases caused by the strictures. Intracranial pressure measurements in CCSVI subjects, to the best of our knowledge, do not currently exist. We note however that for the IIH condition associated to dural sinus anomalies, invasive pressure measurements do actually exist.[19,20] These dural sinus pressure measurements show the expected venous sinus hypertension. Pressure measurements in other districts, *e.g.* deep cerebral veins and inner ear fluids, resulting from intracranial or extracranial strictures in humans are, to the best of our knowledge, not available. It is here where mathematical models may also prove useful; potentially, they could provide quantification of relevant haemodynamical variables, including pressure.

In the context of disturbed brain haemodynamics, Müller and Toro[21] proposed the first global, closed-loop multiscale mathematical model to study this phenomenon. In this model, the geometry for the cerebral and extracranial venous system is individually defined by means of segmentation of patient-specific MRI data. The model was later enhanced[22] to include one intracranial compartment and Starling resistors to better describe the physiology of cerebral veins, CSF dynamics, and to more fully account for the interaction of fluid compartments in the CNS. See also the related work of

Caiazzo et al.[23] The enhanced global model of Müller and Toro[22] has been used to study the effect of extracranial venous stenoses on intracranial haemodynamics by Müller et al.[24] the effect of venous valve malfunction on cerebral haemodynamics[25] and to produce some preliminary results on CCSVI and sudden sensorineural hearing loss.[26] In these studies, it is demonstrated that disturbed brain haemodynamics and intracranial venous hypertension occur as a result of extracranial strictures in the neck veins and the AV. For a review on these works in the broader context of neurological diseases potentially related to extracranial venous anomalies, see the review paper by Toro.[27]

In the present work, we extend the global model of Müller and Toro[21,22] to include submodels for the inner ear circulation. Then we apply the extended model to study the fluid dynamics resulting from the CCSVI condition, with special attention given to the inner ear haemodynamics. Prior to the specific study of inner ear circulation we perform in vivo validation of the extended global circulation for a specific, healthy subject. Comparison of computed and MRI measured blood flow is shown; the results are satisfactory. The study of pathological cases then follows by investigating the altered fluid dynamics resulting from extracranial venous strictures. Our results show that extracranial outflow venous strictures impede efficient cerebral venous drainage, alter blood flow dynamics, increase CSF pressure and cause chronic venous hypertension throughout the cerebral venous system, including the inner ear circulation.

The theoretical contribution of the present paper is in line with both extracranial venous strictures and altered intracranial dynamics, as will be discussed later. The rest of this paper is structured as follows. After a section on materials and methods we present our results, which include a validation exercise on a healthy subject and two anomalous cases, namely extracranial venous stenosis and anomalous venous valves. There follows a discussion of results. Supplementary material is presented in the Appendix.

Materials and Methods

In this paper we extend the global, closed-loop, multiscale mathematical model proposed by Müller and Toro[21,22] to include submodels for the inner ear circulation. The original model contained 1D, cross-sectional area averaged equations for 85 major arteries and 188 major veins, as well as 0D compartmental models for microcirculation beds,[28] the heart,[29] the pulmonary circulation[29] and the CSF.[30] The model also includes submodels for valves in the venous system.[25,31] The 1D model describes the space (x) and time (t) variation of vessel cross-sectional area $A(x,t)$, blood flow rate $q(x,t)$ and pressure $p(x,t)$. Starling resistors are used in the cerebral venous system to obtain a more realistic description of the haemodynamics in the main regions of interest. In the original model, the vessel geometry for the main arteries and veins of the body is mostly obtained from the literature, while MRI data from specific subjects are used to describe the major cerebral and extracranial venous vessels. See Utriainen et al.[32] for a detailed description of the acquisition process of the MRI data.

For the purpose of investigating the influence of extracranial venous obstructions on the inner ear circulation we have extended the Müller-Toro model[21,22] by adding inner-ear vessels to the global network, utilising data from the literature.[33-35] The anterior inferior cerebellar artery, branching from the basilar artery, is added to account for the inner-ear arterial blood supply. To account for inner-ear venous drainage we have incorporated 1D representations for the LABV and the VCAQ. LABVs transport blood from the inner ear venules and empty at the insertion of the transverse sinus into the sigmoid sinus. VCAQs, instead, are directly connected to the superior bulbs of the IJVs. Moreover, two 0D compartments accounting for the inner ear microcirculation were also inserted into the original vascular network. Figure 1 gives a detailed illustration of the cerebral and extracranial venous network implemented in the present version of the model.

Results

Here we use the term CCSVI condition in a generic sense to include a wide range of extracranial venous malformations, such as stenosis, hypoplasia, atresia and stenotic or regurgitant venous valves. The anomalies considered in this paper are stenoses and stenotic valves in the IJVs and the AV; these are the most frequently found anomalies in CCSVI diagnosed subjects. In this section we first carry out an in vivo validation of the entire model for a healthy control, comparing computed results against in vivo MRI measurements. Then we simulate pathological cases, which is the main subject of this paper.

Healthy control

An in vivo validation of the complete model for a healthy subject in supine position is performed here. Figure 2 depicts computed profiles (full line) for pressure and flow, over a cardiac cycle. The second column shows computed pressure, while the third column shows both computed (line) and MRI-measured values for flow (symbols). The comparison between computed and measured values for flow is satisfactory, considering the complexity of the full problem and the modelling simplifications adopted; the agreement is satisfactory both from the point of view of flow average values over the cardiac cycle as well as the waveforms. For pressure, there are no measured values available in the literature, as far as we are aware. Recall that pressure measurement is an invasive procedure. However, some estimates can be found in the literature. Such estimates are close to the values computed by our model. For example, Schaller[36] estimates an average value of p=6.6±2 mmHg for blood pressure at the confluence of sinuses; our model predicts an averaged value over the full cardiac cycle of p=6.5 mmHg. More in vivo validation results are available but are not included here. The MRI measurements used for the validation are reported in Müller et al.[24] Next, we deal with simulation of pathological cases.

Extracranial venous stenosis

Here we apply our mathematical model to simulate the haemodynamics resulting from anomalous extracranial venous strictures. We consider a vessel to be stenotic if a significant narrowing of its cross-sectional area is present. In this work, stenoses are represented as a 2 cm long vessel segment whose equilibrium cross-sectional area $A^s_0(x)$ is restricted as follows: $A^s_0(x) = 0.1\ A_0(x)$, where $A_0(x)$ is the normal equilibrium cross-sectional area of the vessel of interest. In the present study we consider two CCSVI cases defined by Zamboni et al.,[2] namely cases A and B, schematically represented in Figure 3. Case A includes a stenosis in the left IJV, above the insertion of the middle thyroid vein, and a stenosis in the AV, close to the azygos arch. Case B is like case A, except that the right IJV is also stenosed, symmetrically with respect to the left IJV. The presence of strictures in the IJVs and the AV causes significant alterations to the normal haemodynamics in the cerebral venous network and in the main blood drainage routes towards the heart, as we shall demonstrate.

We first consider the effect of local stenoses on the haemodynamics of extracranial vessels, namely IJVs and AV. Figure 4

shows computed results for the haemodynamics across the stenoses in both IJVs. The first column depicts the locations of interest, while the second and third columns show computed pressure and venous blood flow, as functions of time, within one cardiac cycle. Results are shown for the healthy control and for the two anomalous cases A and B. Cardiac-cycle averaged values are displayed in squared brackets.

As expected, a very consistent reduction of venous blood flow in the stenotic vessels is observed. In case B for example, bottom row of Figure 4, the left IJV blood flow decreases from 10.08 mL s^{-1} in HC to 3.74 mL s^{-1}, a reduction of about 65%. Also, a sizeable increase in venous blood pressure jump Δp across the stricture is observed, namely $\Delta p \approx 1.5$ mmHg, which is about the 25% higher than in the healthy control; this computed result is consistent with measured values reported by Zamboni *et al*.[2] Furthermore, the literature, *e.g.* Zamboni *et al*.[2] have reported another typical haemodynamical disturbance caused by the CCSVI
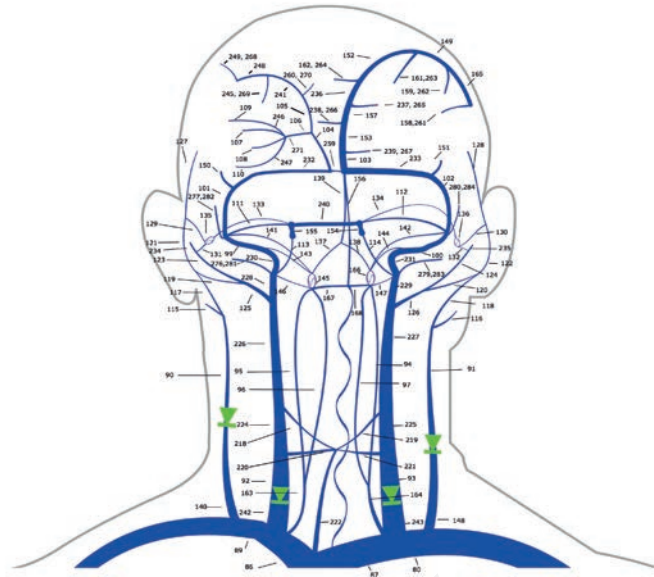
Figure 1. Properties of all the 1D arteries and veins not included in Appendix Table 1, see Müller and Toro.[29,30] Triangles (green) represent location of venous valves in both internal jugular veins (IJVs) and external jugular veins (EJVs), included in Appendix Table 1, see Müller and Toro.[21,22] Triangles (green) represent location of venous valves in both internal jugular veins (IJVs) and external jugular veins (EJVs).
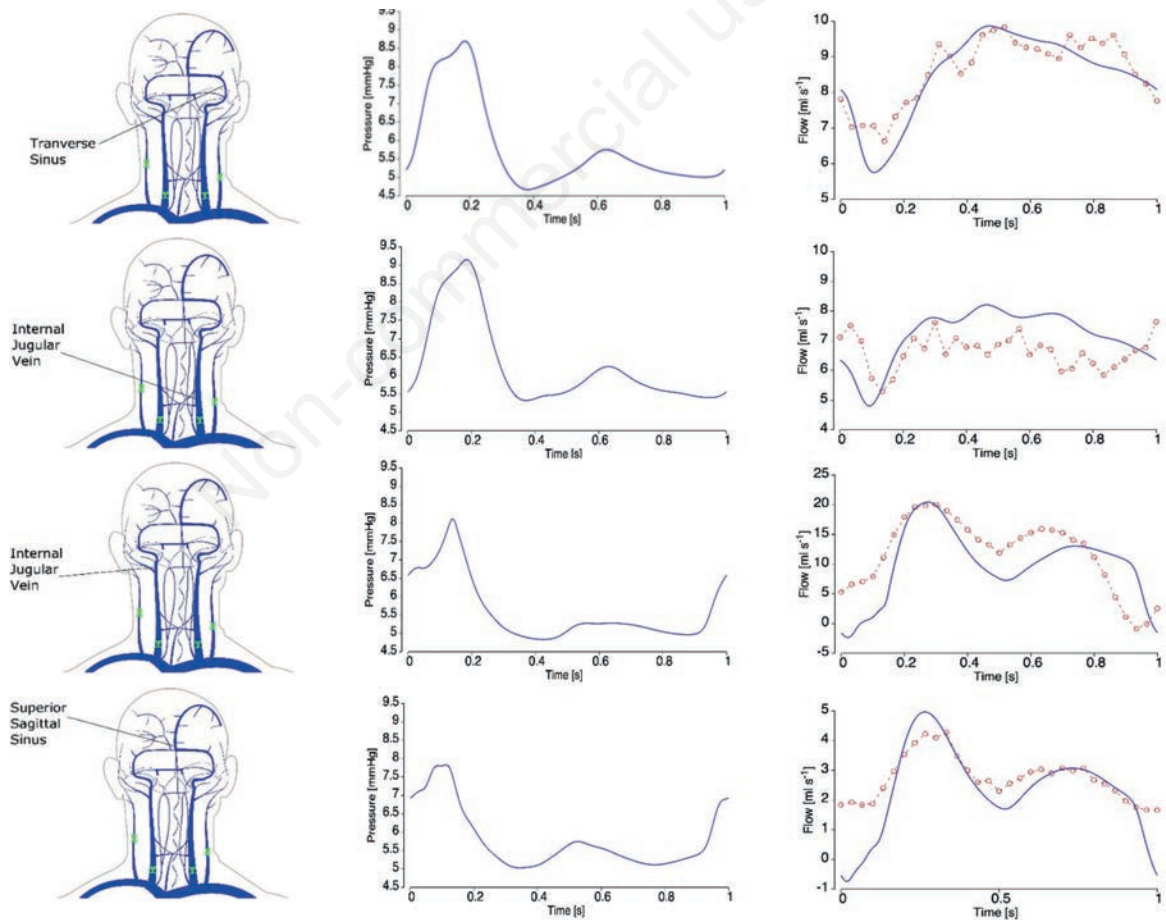
Figure 2. *In vivo* validation for healthy control. The left column shows the spatial locations on the vessels of interest in the modelled venous network; the middle column shows computed pressure at various locations as function of time for one cardiac cycle; the right column compares the corresponding computed (full line) venous blood flow against the MRI flow measurements (*symbols*). No measured data for pressure is available.

condition, that is, redirection of blood flow, in the direction of alternative extracranial routes. This empirical observation is also reproduced by our mathematical model. From the IJVs, blood is mainly redirected towards the external jugular veins (EJVs) via the common facial veins. This results in increased venous blood flow, up to four times that of the HC, in the external jugular (EJV) adjacent to the stenosed IJV. A corresponding pressure rise of about 0.6 mmHg in the EJV is also observed (not shown here). Another common consequence of the CCSVI condition, as shown by our model, is the redirection of blood from one side to the other, in case of unilateral stenoses in the IJV (as in case A). Many vessels con-
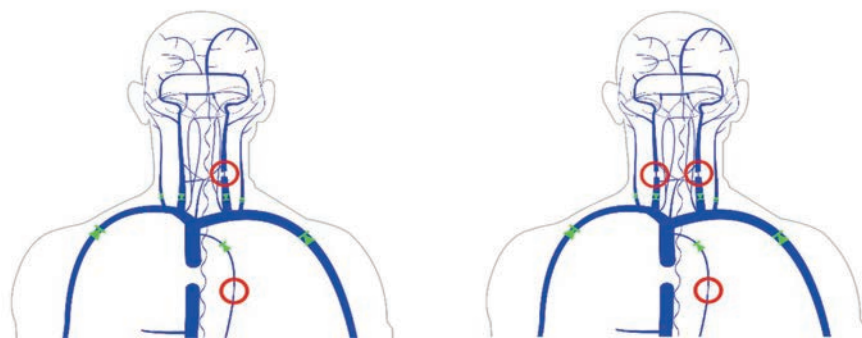
Figure 3. Extracranial venous stenoses. Venous stenoses in the present mathematical model are depicted by red circles. Two cases are considered: case A (left) and case B (right) taken from 2.
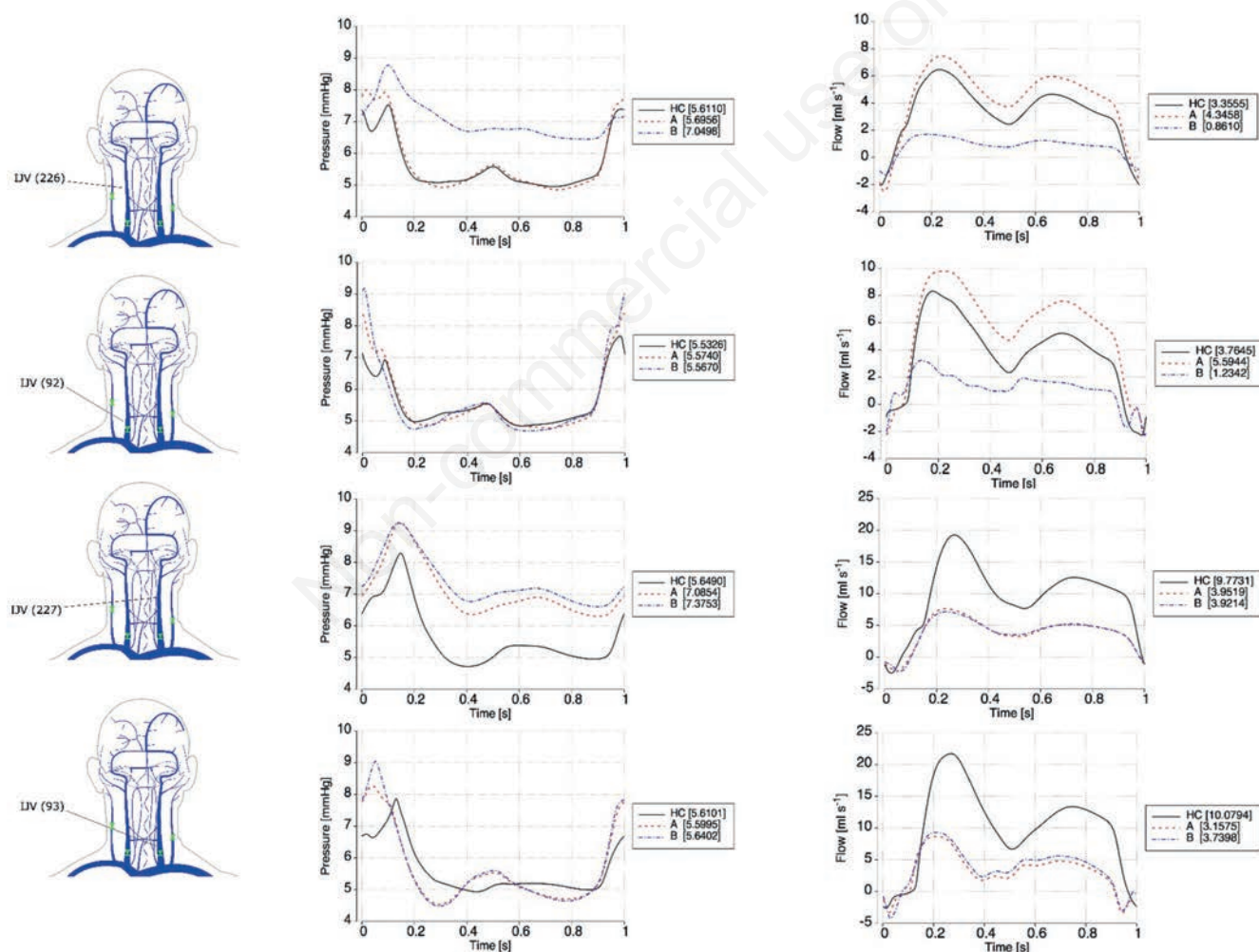
Figure 4. Extracranial venous stenoses. Computed results for pressure and venous blood flow in extracranial venous vessels for one cardiac cycle, at two locations in IJVs, upstream and downstream of the stenoses. Three model simulations are shown: healthy control (HC: continuous line) and the two pathological cases A (dashed line) and B (dashed and dotted line). The left column shows the location of the points of interest in the venous network, the central column shows venous blood pressure and the right column shows venous blood flow, all as functions of time within one cardiac cycle. Numbers in brackets in legends represent the average of the computed quantity over one cardiac cycle. Vessel numbering is consistent with.[21,22]

tribute to transport this blood, such as inferior and superior petrosal sinuses, intra-cavernous sinus, marginal sinuses and lateral anterior condylar veins (not shown here).

Figure 5 depicts the computed haemodynamics in the inner-ear vein vessel segments located upstream of the Starling resistor. No clear differences in blood flow between the healthy control and the pathological cases are seen; this is presumably due to the fact that these vessels are just connected to 0D models and deliver to the venous network. Pressure, however, is substantially increased in the presence of stenoses; in fact the pressure increment is comparable to that for the IJVs in the pathological cases, as seen in Figure 5 for segments 226 and 227; results for other neighbouring segments are not shown.

Figure 6 shows cardiac-cycle averaged pressures in selected vessels. The left panel shows a comparison of computed cardiac-cycle averaged pressures for the HC and the two pathological cases A and B, in the following five venous vessels: superior petrosal sinus (SPS), inferior petrosal sinus (IPS), transverse sinus (TS), superior sagittal sinus
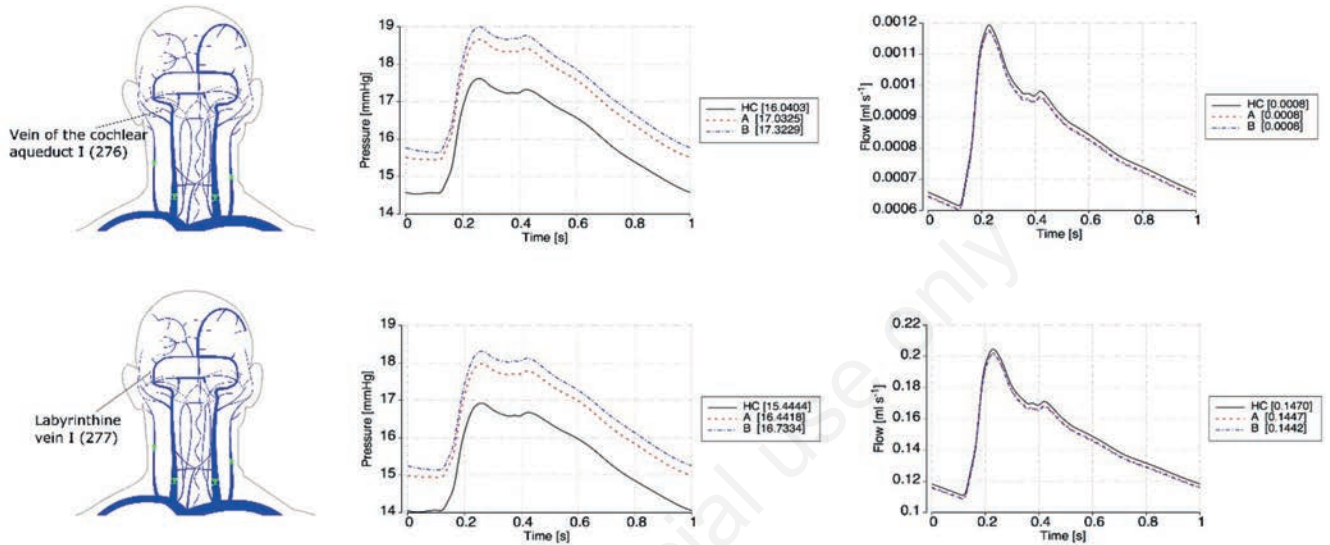
Figure 5. Extracranial venous stenoses. Computed results for the right inner ear veins. Three model simulations are shown: the healthy case (HC: continuous line) and the pathological cases A (dashed line) and B (dashed and dotted line). The left column shows the location of the vessel of interest in the venous network, the central column shows blood pressure and the right column shows venous blood flow rate. Numbers in square bracket represent the average of the computed quantity over the cardiac cycle.
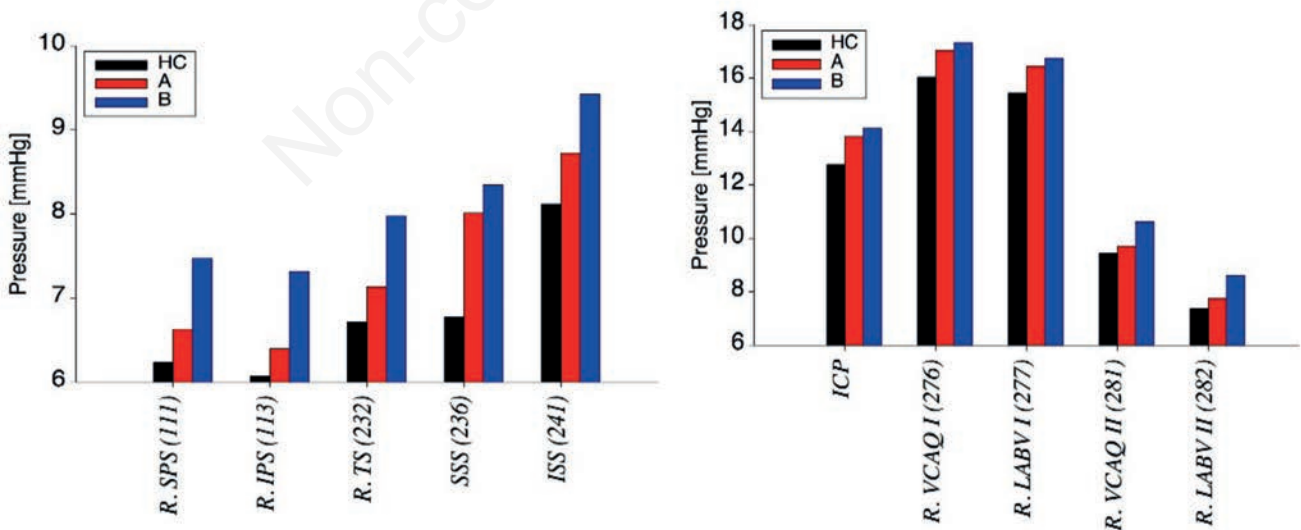
Figure 6. The two panels represent the computed cardiac-cycle averaged pressures in case of extracranial venous stenoses. Left panel summarizes the results in the main dural sinuses of the venous network. SPS: superior petrosal sinus, IPS: inferior petrosal sinus, TS: transverse sinus, SSS: superior sagittal sinus and ISS: inferior sagittal sinus. (Vessel numbering is consistent with 21,22). Right panel summarizes the results in intracranial compartment and veins of the right inner ear. ICP: intracranial compartment, VCAQ: vein of the cochlear aqueduct, LABV: labyrinthine vein. For each vessel and location, the left bar corresponds to the healthy control (HC), the middle bar refers to the pathological case A and the right bar to the pathological case B.

(SSS) and inferior sagittal sinus (ISS). It is seen that the pressure rise generated by the extracranial venous strictures is transmitted back to the intracranial circulation and is computed to be around 1.5 mmHg. However, a corresponding variation of flow is not obvious in these vessels, as blood cannot exploit collateral vessels, as was the case in the IJVs. Blood pressure of the SSS is particularly important, as reabsorption of CSF into the venous vasculature depends linearly on the pressure difference between the intracranial compartment and the SSS.[21,30] Therefore, higher blood pressure in SSS leads to reduced CSF reabsorption, increased CSF pressure and intracranial hypertension. Right panel of Figure 6 shows a comparison of computed cardiac-cycle averaged pressures for the HC and the two pathological cases A and B, in the intracranial compartment (intracranial pressure, ICP) and the inner ear veins considered in this study, namely the VCAQ and the LABV.

Our mathematical model assumes that the intracranial pressure ICP acts as the external pressure on cerebral veins and inner ear veins. Starling resistors are introduced in the middle of all the cerebral veins, as well as in the inner ear veins. Part of the function of Starling resistors is to prevent automatic backward transmission of pressure waves from external vessels up to the terminal intracranial veins and to prevent cerebral venous collapse due to the action of intracranial pressure. Hence, the observed venous hypertension in the inner ear veins is not directly caused by the backward transmitted pressure waves from the obstructed sites, as occurs in the dural sinuses, but is originated by its external pressure increase (ICP). Indeed, this could be seen explicitly from the tube law:[21,22] a higher external pressure acting on the vessel wall induces a higher internal pressure in the same vessel. Moreover, it is worth noting that in the inner ear veins, as well as in the intracranial compartment, the pressure increment from the HC and the pathological cases is not significantly different from the respective increments in the dural sinuses.

This concludes the study of the effect of extracranial venous stenosis on brain haemodynamics and on inner ear circulation in particular. Next we study the effect of another kind of extracranial venous anomaly, namely stenotic venous valves.

Stenotic venous valves

The presence of valves in the human jugular veins has long been established, starting from cadaveric dissection studies, even though their anatomy, prevalence and competence are still the ongoing subject of studies.[36] Valves in jugular veins are meant to ensure one-way venous blood flow and, apart from stenotic malformations, are the only structures that may modify such venous blood flow as well as pressure wave propagation between the brain and the right atrium. It is therefore reasonable to suppose that valve malfunction may have an effect on intracranial venous haemodynamics. As a matter of fact, Toro and collaborators[25] found that valve function has a visible effect on intracranial venous haemodynamics, including dural sinuses and deep cerebral veins. They reported that valve obstruction causes venous reflux, redirection of flow and intracranial venous hypertension. Two modes of valve functioning were identified in their model,[25] namely obstructed or stenotic valves, which cannot reach total opening, and incompetent valves, which cannot reach total closure. They also reported that valve *incompetence* leads to small alterations of pressure within intracranial veins, while *valve obstruction* can have more visible effect, depending on the degree of obstruction. Obstructions greater than about 75% produce substantial pressure increases, above which the pressure increase grows very sharply with the degree of occlusion. In the study of Toro and collaborators,[25] the mathematical model used did not include a detailed inner ear circulation network and was therefore not applicable to the topic of concern in the present paper.

It is reasonable to suppose that the same mechanism regarding stenoses and the results reported in [37] could be relevant. We may therefore hypothesize that valve malfunctioning would generate pressure increases that would be transmitted up to the intracranial compartment, and to the inner ear circulation. That is, valve incompetence may be a cause for venous blood pressure rise around the inner ear. For the present study we considered two cases of stenotic valves that cannot attain full opening, named case C and case D (Figure 7). Case C is characterised by a stenotic valve in the left IJV, while case D considers stenotic valves (symmetric) in both left and right IJVs. Valves are located in the proximal segment of the vein, downstream of the location of the stenoses considered in cases A and B in the previous section on vein stenosis. In both cases a valve obstruction of 75% of the reference cross-sectional area was assumed, when the valve has achieved its maximum opening. Figures 8 and 9 show our computed pressure and venous flow in the IJVs and in the inner ear veins, respectively. The results show the same tendency as those for stenotic veins of the previous subsection, though in general the variation in haemodynamical quantities is less pronounced. The histograms of Figure 10 summarise the cardiac cycle averaged pressures in the main dural sinuses, in the intracranial compartment and in the inner ear veins. As for the stenosed vessels, a pressure rise is originated in the IJVs upstream of the stenotic valves, and is transmitted up to the dural sinuses, into the intracranial compartment and deep cerebral veins. Also in this case, the increased external pressure acting on the inner ear veins produces a venous blood pressure rise in the inner ear circulation. Essentially, a stenotic valve restricts the amount of outflowing blood from the brain and thus it reproduces the behaviour associated to a venous stenosis. In cases C and D we have considered a constriction of 75%, and the pressure rise observed is less severe than that of cases A and B. In fact the
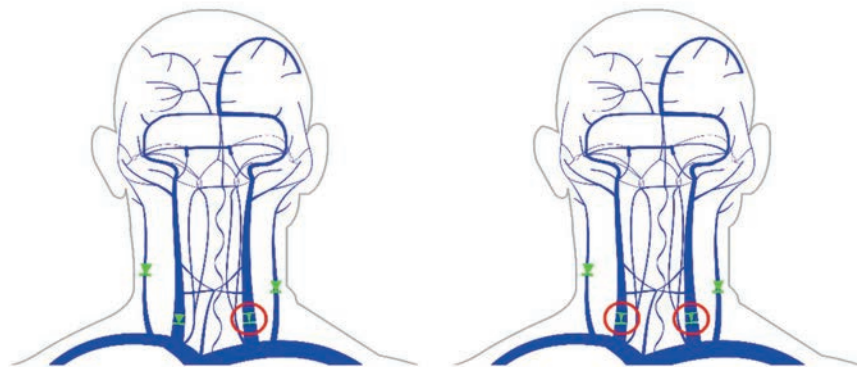
Figure 7. Stenotic venous valves. Valves are represented by green triangles and are present in both IJVs and EJVs. The pathological cases characterized by stenotic valves are represented by red circles: cases C (left) and D (right).
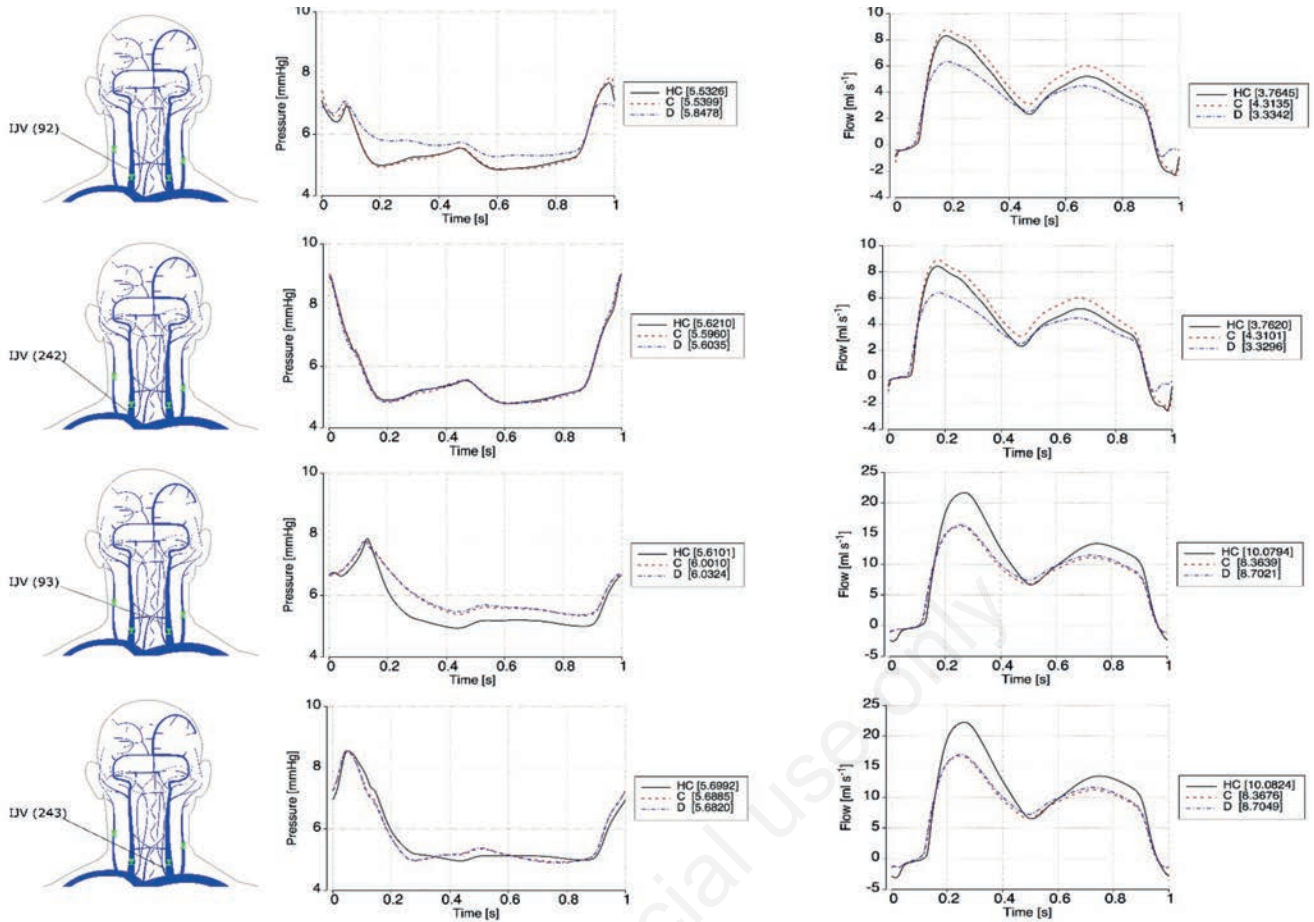
Figure 8. Stenotic venous valves. Computed results for two locations of each IJV, one upstream and one downstream the stenotic valve. The left colum shows vessel locations of interest, the middle colum shows computed pressure and the right column shows computed venous blood flow. Three model simulations are shown: the healthy case (HC: continuous line) and pathological cases C (dashed line) and D (dashed and dotted line). Numbers in square brackets in the legends represent the average of the computed quantity over the cardiac cycle. Vessel numbering is consistent with [21,22].
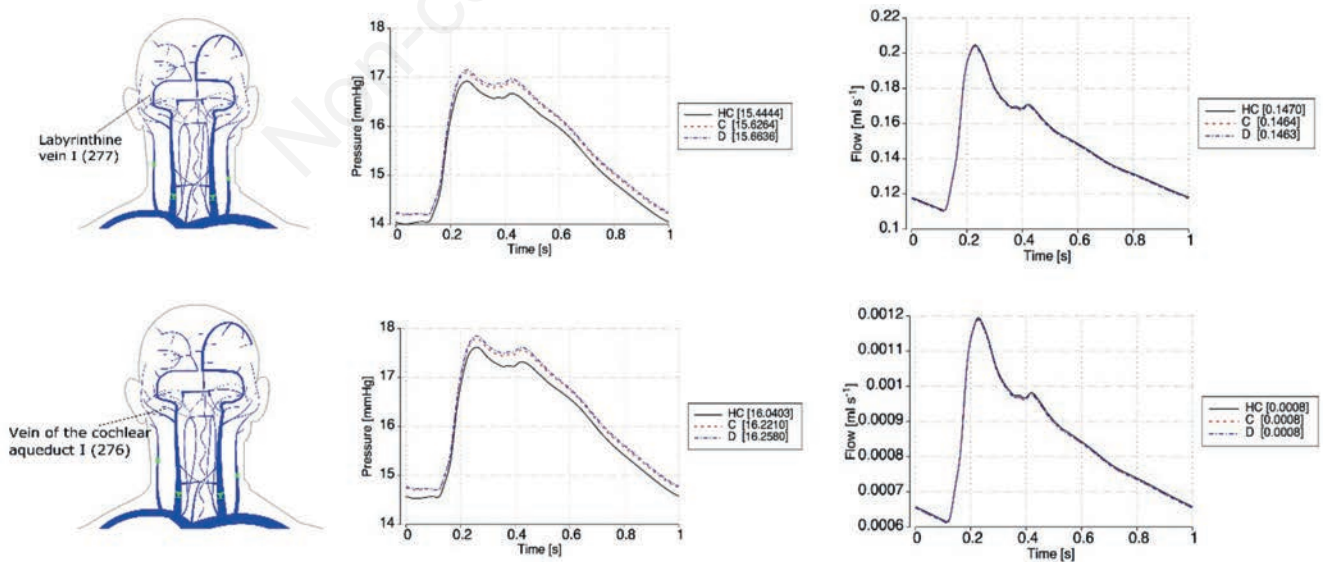
Figure 9. Stenotic Venous Valves. Computed results for the right inner ear veins. The left colum shows vessel locations of interest, the middle colum shows computed pressure and the right column shows computed venous blood flow. Three model simulations are shown: the healthy case (HC: continuous line) and the pathological cases C (dashed line) and D (dashed and dotted line). Numbers square brackets in legend represent the average of the computed quantity over the cardiac cycle.

difference in pressure jump across a stenotic valve between the healthy control and the pathological cases C and D is about $\Delta p \approx 0.3$ mmHg. As noted in [25], the haemodynamical effect of the degree of valve occlusion rises sharply from about 75%. This means that the case considered here is that of a low-degree valve occlusion and therefore its effect on venous hypertension is less marked than in the case of venous stenoses. Also to be noted is the fact that the AV has normally a very small cross-sectional area, and therefore its obstruction does not visibly influence the results. Moreover, we also note that valves are located below the segments of the IJVs that are stenosed in cases A and B. This means that blood blocked by the stenotic valves can exploit a larger number of collaterals to allow blood flow towards the heart. Therefore a smaller amount of blood is collected above the valve, thus a smaller pressure rise is observed.

A comment on CSF pressure, intracranial hypertension and CSF reabsorption is in order. Figure 10, right frame, includes results for ICP, the pressure in the CSF compartment. ICP increases in the presence of extracranial venous strictures, even if such increases are modest. Our computations show, details omitted, that this is a consequence of increased venous pressure in SSS, thereby hampering CSF reabsorption and thus favouring CSF accumulation. We emphasise that the present version of our global model adopts a single 0D model for the entire CSF compartment. This is indeed a limitation of the model, as its local resolution, in the inner ear zone for example, would be poor, though still retaining the trend.

Discussion and Conclusions

The reported work in the present paper falls within a wider recently started research effort aimed at studying cerebral venous flow in humans. In particular, the potential consequences of disturbed cerebral venous outflow, broadly represented by CCSVI.[2] Here CCSVI is interpreted as involving several anomalous patterns of malformations in the neck veins and/or in the AV, including venous valve anomalies, that perturbs cerebral venous outflow. Besides MS and MD, several other neurological diseases have been hypothesized to be related to CCSVI, such as bilateral sudden sensorineural hearing loss[38] (SSNHL), transient global amnesia (TGA),[39] retinal abnormalities[40] and idiopathic Parkinson's disease.[41] See [27] for a review. The lack of simple and non-invasive techniques capable of measuring intracranial venous pressure has revealed the necessity of alternative methods to examine the effects of strictures on the cerebral venous circulation. The development of mathematical models for the circulation certainly provides promising tools for this kind of research, but not without its own limitations. A major difficulty is the vast intersubject variability, particularly in the venous district, which prevents the adoption of a universal description for a human body. The variability of the head and neck venous system has been demonstrated through the years, in terms of vessel dimensions and geometry; depending on these factors, blood main routes toward the heart can be very different from one individual to another. See, for example, Doepp et al.[42] for a large study on the most common extracranial routes in the supine position; see Valdueza et al.[43] for the rearrangement of blood outflow paths in an individual under change of posture. Our mathematical model uses detailed patient-specific geometry of the head and neck venous network obtained by means of MRI techniques.

In this paper we have established two interrelated consequences of CCSVI-like anomalies, namely i) intracranial venous hypertension, with disturbed inner ear circulation and inner-ear venous hypertension and ii) increased CSF pressure and associated intracranial hypertension. Previous studies have tended to decouple the roles of the venous and CSF compartments, when in fact their fluid dynamics and physiology are intimately linked. Several reported animal experiments are based on injection of artificial CSF to raise intracranial pressure. In our model, intracranial hypertension and intracranial venous hypertension are the physiological consequence of increased intracranial venous volume due to extracranial venous outflow strictures; increased
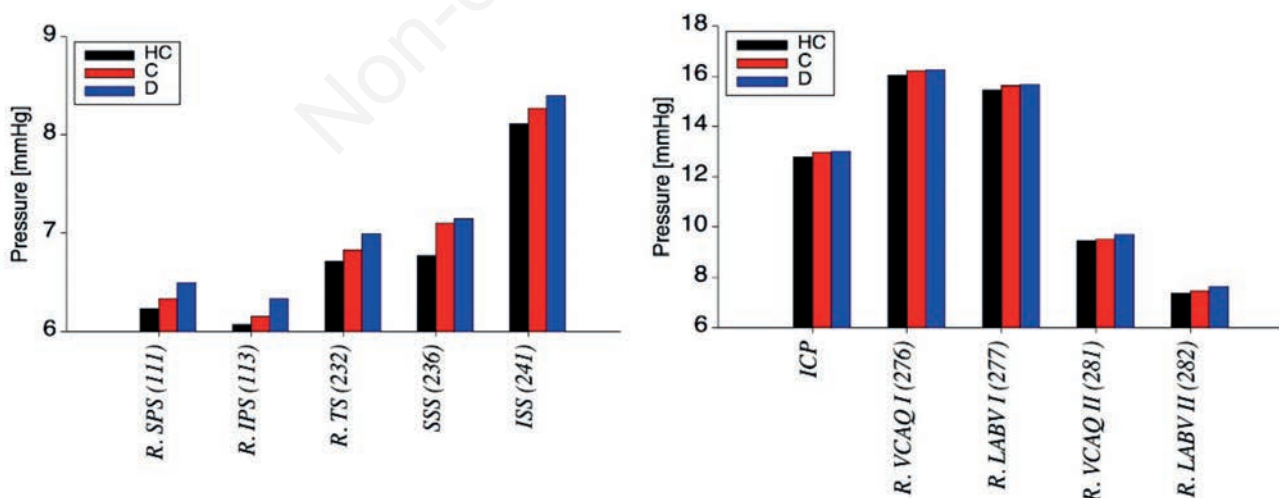
Figure 10. The two panels represent the computed cardiac-cycle averaged pressures in case of stenotic venous valves. Left panel summarizes the results in the main dural sinuses of the venous network. SPS: superior petrosal sinus, IPS: inferior petrosal sinus, TS: transverse sinus, SSS: superior sagittal sinus and ISS: inferior sagittal sinus. (Vessel numbering is consistent with [21,22]**). Right panel summarizes the results in intracranial compartment and veins of the right inner ear. ICP: intracranial compartment, VCAQ: vein of the cochlear aqueduct, LABV: labyrinthine vein. For each vessel and location, the left bar corresponds to the healthy control (HC), the middle bar refers to the pathological case C and the right bar to the pathological case D.**

venous pressure hampers CSF reabsoption leading to increased CSF pressures.

Inner-ear venous hypertension has for a long time been regarded as a hallmark of MD.[8,9,14-16,44] In the animal experiments of Friis and Qvortrup [8] they blocked the venous flow in the VVA that drains into the sigmoid sinus. They visualized the reversed venous blood flow direction (reflux) in the extraosseous part of the vein. They argued that reversed venous flow in the VVA toward the inner ear could potentially cause portal circulation in the inner ear, with a range of potential consequences, including risk of thrombosis, local hypoperfusion and accumulation of neurotoxic materials. In the present work the blockage was performed in humans in the extracranial veins, leading to analogous observations, including reversed flow and venous hypertension.

Our second result regarding increased CSF pressure is perhaps more appealing in trying to understand the mechanisms at work. Subarachnoid spaces and thus CSF are directly in contact with the perilymphatic space through the cochlear aqueduct. Increases in CSF pressure are transmitted directly and rapidly to the perilymphatic space, as demonstrated by the early animal experiments of Carlborg and Farmer.[44] There is evidence that CSF pressure increases are also transmitted, even if more slowly, to the endolymphatic space via the endolymphatic sac and endolymphatic duct. A key issue is the pressure difference $\Delta P_{Reiss} \neq 0$ (in absolute value) across the endolabyrinthine membrane (the Reissner membrane) between the endolymphatic space and and perilympahtic space. While many investigators consider to be incompatible under physiological conditions, there are many investigations in which, even if small, a pressure difference is found *e.g.*[45] Some authors have suggested that ΔP_{Reiss} in the range 1.4 to 3.5 mmHg would lead to rupture of the endolabyrinthine membranes.[44]

At this stage it is worth noting the electrolyte levels of perilymph and endolymph. Sensory and neural structures are normally bathed in perilymph, which has electrolyte levels similar to CSF, suitable for neural transmission. Moreover, the potassium level of endolymph is toxic to sensory and neural structures and blocks neural excitation and transmission.[16] On the other hand, histological studies suggest that the acute vertiginous episodes are caused by potassium intoxication following ruptures of the membranous labyrinth. Schuknecht[16] described the pathophysiology of *endolymphatic hydrops*, whose cause he ascribes to the occlusion of the endolymphatic duct and that the sudden onset of vertigo episodes is

acute vestibular paralysis caused by potassium intoxication following a rupture of the endolymphatic system. Vertigo episodes have limited time duration, due to the healing capacity of the membranous labyrinth, whose ability to repair itself has been demonstrated in animal studies.

Our theoretical results are consistent with the above observations and with the animal experiments of Yoshida and Uemura,[18] in that hypertension is also observable in other fluids in the inner ear, in the perilymphatic and endolymphatic spaces. As already indicated, the perilymphatic space has a relatively free communication with the subarachnoid space via the *cochlear aqueduct*, through which CSF pressure waves are transmitted. The *endolymphatic sac* and the *endolymphatic duct*, on the other hand, would also transmit CSF pressure waves to the endolymphatic space that in theory would equilibrate pressure across the interface between the endolymphatic space and the perilymphatic space, the Reissner membrane. According to these authors,[18] both the endolymphatic and perilymphatic pressures rise linearly and proportionally to ICP increment, and that a pressure rise in the CSF space is associated to an analogous pressure rise in both inner ear fluid spaces. No significant time lag was observed between the CSF pressure rise and the alteration of the inner ear fluids. Moreover, no hydrostatic pressure gradient was observed between the two inner ear spaces, though this result is at variance with the previously mentioned studies. The experiments in[18] suggest that a chronic elevation of the CSF pressure due to the extracranial venous occlusions would result in a chronic elevation of the endolymphatic and perilymphatic pressures. From their measurements, a linear relation is observed between the CSF pressure increase and the endolymphatic pressure increase, with slope $m = 0.89$. A similar behaviour is observed between ICP and perilympahtic pressure, with slope $m = 0.84$. They argue that the slopes should be $m = 1.0$ and that experimental details prevented this from happening. Assuming their experimental finding is correct, our computed CSF pressure rise $\Delta P_{csf} \approx 1.3$ mmHg in our case B may result, with good approximation, in an increment of $\Delta P_{end} \approx 0.3$ mmHg in the endolymphatic space and an increment of $\Delta P_{per} \approx 1$ mmHg in the perilymphatic space.

Another aspect of the experimental work in[18] is the effect of CSF pressure rise on the hearing function. To that end, they measured the cochlear microphonic (CM); this is an electric signal generated by the hair cell movement, which is proportional to the displacement of the basilar mem-

brane, a structure of the inner ear responsible for the transduction of sound waves into an electric signal. This displacement is thus proportional to the amplitude of the signal sent to the brain. The authors observed a reduction of the CM intensity, which they ascribed to the decreased cochlear blood flow. A clear consequence of this behaviour was that a low acoustic stimulus was not longer recognized and thus the hearing threshold was raised, in the case of a high CSF pressure. Furthermore, the mechanism was shown to be reversible, so that the normal acoustic function was restored when CSF pressure was set back to normal values. We note that their observations were associated to very high values of CSF pressure. Such high values cannot be reached in a CCSVI subject on a supine position alone, unless additional factors come into play, such as sudden postural change, Valsalva type manoeuvres or external compression of the head.

In a study conducted by Valk *et al.*,[37] endolymphatic hydrops was induced in guinea pigs by inserting artificial endolymph in the endolymphatic space and thus causing inner ear pressure rise consistent with the increments observed in our simulations. The experiments of Silverstein[17] support the theory that the onset of vertigo episodes follows the rupture of the membranous labyrinth. He injected artificial endolymph into the perilymphatic space in cats, thus producing a sudden increase in the potassium concentration of the perilymphatic fluid, which is what would happen in the actual rupture of the membranous labyrinth. In reality, after the membrane rupture, potassium ions are pushed towards the perilymphatic space by the osmotic pressure gradient, thus reducing its electric potential and blocking the neural structures, and thus reducing the hearing function.

Promising biophysically based therapies have recently been put forward; see for example the works of Bruno and collaborators.[5,6] The present work is a contribution to the study of the basic underlying mechanisms that may explain the encouraging results of these therapies, though much work is still needed. A limitation of the present work is that the simulations were carried out for a subject in the supine position. Some challenging algorithmic problems need to be resolved in order to simulate postural changes. These are the subject of current investigations. Another limitation is the representation of the CSF compartment. The current version assumes a single CSF compartment; this is indeed too simple. Current developments (Toro EF, *et al*. Holistic multi-fluid mathematical model for

the central nervous system; 2017 - data not published) assume a more detailed CSF model that includes the four cerebral ventricles, where CSF is actually produced, the aqueduct of Sylvius, the cerebral subarachnoid space, the spinal subarachnoid space and the brain parenchyma.[46] Another possible future extension would be the construction of a submodel for the inner ear that includes the endolymphatic and the perilymphatic spaces, in order to analyse in more detail the pressure variations of these fluids as a result of CSF pressure rise.

References

1. Alperin N, Lee SH, Mazda M, et al. Evidence for the importance of extracranial venous flow in patients with idiopathic intracranial hypertension (IIH). Acta Neurochir 2005;95:129-32.

2. Zamboni P, Galeotti R, Menegatti E, et al. Chronic cerebrospinal venous insufficiency in patients with multiple sclerosis. J Neurol Neurosurg Psychiatry 2009;80:392-99.

3. Alpini DC, Bavera PM, Hahn A, et al. Chronic cerebrospinal venous insufficiency (CCSVI) in Ménière's Disease. Case or cause? ScienceMED 2013;4:9-13.

4. Alpini DC, Bavera PM, Di Berardino F, et al. Bridging the gap between chronic cerebrospinal venous insufficiency and Ménière disease. Veins and Lymphatics 2016;5:5687.

5. Bruno A, Califano L, Mastrangelo D. Chronic cerebrospinal venous insufficiency in Ménière's Disease: diagnose and treatment. Veins and Lymphatics 2014;3:3854.

6. Bruno A, Napolitano M, Califano L, et al. The prevalence of chronic cerebrospinal venous insufficiency in Ménière's disease: 24-month follow-up after angioplasty. J Vasc Interv Radiol 2017;28:388-91.

7. Di Berardino F, Alpini DC, Bavera PM. Chronic cerebrospinal venous insufficiency in Ménière's disease. Phlebology 2014;4:274-9.

8. Friis M, Qvortrup K. A potential portal flow in the inner ear. The Laryngoscope 2007;117:194-8.

9. Friberg U, Rask-Andersen H. Vascular occlusion in the endolymphatic sac in Ménière's disease. Ann Otol Rhinol Laryngol 2002;111:237-45.

10. Gray H, Carter HV. Gray's anatomy: the anatomical basis of clinical practice, 40th edition Edinburgh: Churchill-Livingstone; 2008.

11. Silverthorn DU. Human physiology: an integrated approach, 5th edition. San Francisco: Pearson/Benjamin Cummings; 2010.

12. Moller AR. Hearing: anatomy, physiology and disorders of the auditory system, 2nd edition. Academic Press; 2006.

13. Tassinari MT, Mandrioli D, Gaggioli N, et al. Ménière's disease treatment: a patient-centered systematic review. Audiol Neurotol 2015;20:153-65.

14. Gussen R. Vascular mechanisms in Ménière's disease. Otolaryngol Head Neck Surg 1983;91:68-71.

15. Gussen R. Vascular mechanisms in Ménière's disease. Theoretical considerations. Arch Otolaryngol 1982;108:544-9.

16. Schuknecht HF. Pathophysiology of the endolymphatic hydrops. Arch Otolaryngol 1976;212:253-62.

17. Silverstein H. The effects of perfusing the perilymphatic space with artificial endolymph. Ann Otol Rhinol Laryngol 1970; 9:754-65.

18. Yoshida M, Uemura T. Transmission of cerebrospinal fluid pressure changes to the inner ear and its effect on cochlear microphonics. Eur Arch Otorhinolaryngol 1991;248:139-43.

19. Lazzaro MA, Darkhabani Z, Remler BF, et al. Venous sinus pulsatility and the potential role of dural incompetence in idiopathic intracranial hypertension. Neurosurgery 2012;12:877-84.

20. Raper DMS, Buell TJ, Ding D, et al. A pilot study and novel angiographic classification for superior sagittal sinus stenting in patients with non-thrombotic intracranial venous occlusive disease. J NeuroIntervent Surg 2017 [Epub ahead of print].

21. Müller LO, Toro EF. A global multi-scale mathematical model for the human circulation with emphasis on the venous system. J Numer Method Biomed Eng 2014;30:681-725.

22. Müller LO, Toro EF. An enhanced closed-loop model for the study of cerebral venous blood flow. J Biomech 2014;47:3361-72.

23. Caiazzo A, Montecinos G, Müller LO, et al. Computational haemodynamics in stenotic internal jugular veins. J Math Biol 2014;70:745-72.

24. Müller LO, Toro EF, Haacke EM, et al. Impact of CCSVI on cerebral haemodynamics: a mathematical study using MRI angiographic and flow data. Phlebology 2016;31:305-24.

25. Toro EF, Müller LO, Cristini M, et al. Impact of jugular vein valve function on cerebral venous haemodynamics. Curr Neurovasc Res 2015;12:384-97.

26. Tessari M, Ciorba A, Müller LO, et al. Jugular valve function and petrosal sinuses pressure: a computational model applied to sudden sensorineural hearing loss. Veins and Lymphatics 2017;6:6707.

27. Toro EF. Brain venous haemodynamics, neurological diseases and mathematical modelling. A review. Appl Math Comput 2016;272:542-79.

28. Formaggia L, Quarteroni A, Veneziani A. Cardiovascular mathematics: modeling and simulation of the circulatory system. Milano: Springer-Verlag; 2009.

29. Liang FY, Takagi S, Himeno R, et al. Biomechanical characterization of ventricular-arterial coupling during aging: a multi-scale model study. J Biomech 2009;42:692-704.

30. Ursino M, Lodi CA. A simple mathematical model of the interaction between intracranial pressure and cerebral hemodynamics. J Appl Physiol 1997;82:1256-69.

31. Mynard JP, Davidson MR, Penny DJ, et al. A simple, versatile valve model for use in lumped parameter and one-dimensional cardiovascular models. Int J Numer Method Biomed Eng 2012;28:626-41.

32. Utriainen D, Feng W, Elias S, et al. Using magnetic resonance imaging as a means to study chronic cerebral spinal venous insufficiency in multiple sclerosis patients. Techniques Vasc Intervent Radiol 2012;15:101-12.

33. Chen H, Yu Y, Zhong S, et al. Three-dimensional reconstruction of internal auditory meatus and anatomical study of the inner structures. Zhonghua Er Bi Yan Hou Ke Za Zhi 2000;35:204-6.

34. Habibi Z, Meybodi AT, Maleki F, et al. Superior and anterior inferior cerebellar arteries and their relationship with cerebello-pontine angle cranial nerves revisited in the light of cranial cephalometric indexes: a cadaveric study. Turkish Neurosurgery 2011;21:504-15.

35. Pellet W, Cannoni M, Pech A. Otoneurosurgery. Berlin: Springer, Verlag; 1990.

36. Schaller B. Physiology of cerebral venous blood flow: from experimental data in animals to normal function in humans. Brain Res Rev 2004;46:243-60.

37. Valk WL, Wit HP, Albers FWJ. Evaluation of cochlear function in an acute endolymphatic hydrops model in

the guinea pig by measuring low-level DPOAEs. Hear Res 2004;192:47-56.

38. Alpini DC, Bavera PM, Di Berardino F. Bilateral sudden sensorineural hearing loss and chronic cerebrospinal insufficiency: a case report. Phebology 2013; 28:231-3.

39. Nedelmann M, Eicke MB, Dieterich M. Increased incidence of jugular valve insufficiency in patients with transient global amnesia. J Neurol 2005;252: 1482-6.

40. Adamczyk-Ludyga A, Wrobel J, Simka M, et al. Retinal abnormalities in multiple sclerosis patients with associated chronic cerebrospinal venous insufficiency. Veins and Lymphatics 2012; 1:e2.

41. Liu M, Xu H, Zhong Y, et al. Patterns of chronic venous insufficiency in the major cerebral and extracranial draining veins and their relationship with white matter hyperintensities for patients with Parkinson's disease. J Vasc Surg 2015; 61:1511-20.

42. Doepp F, Schreiber SJ, von Münster T, et al. How does the blood leave the brain? A systemic ultrasound analysis of cerebral venous drainage patterns. Neuroradiology 2004;46:565-70.

43. Valdueza JM, von Münster T, Hoffmann O. Postural dependency of the cerebral venous outflow. Lancet 2000;355:200-1.

44. Carlborg BIR, Farmer JC. Transmission of cerebrospinal fluid pressure via the cochlear aqueduct and endolymphatic sac. Am J Otolaryngol 1983;4:273-82.

45. Weille FL, O'Brien HF, Clark L, et al. Pressures of the labyrinthine fluids. Ann Otol Rhinol Laryngol 1961;70:528-40.

46. Linninger AA, Xenos M, Sweetman B, et al. A mathematical model of blood, cerebrospinal fluid and brain dynamics. J Math Biol 2009;59:729-59.